

High frequency of inactivating tetraspanin *CD37* mutations in diffuse large B-cell lymphoma at immune-privileged sites.

Suraya Elfrink,^{1,*} Charlotte M de Winde,^{1,*} Michiel van den Brand,^{2,*} Madeleine Berendsen,² Margaretha GM Roemer,³ Frank Arnold,¹ Luuk Janssen,¹ Alie van der Schaaf,¹ Erik Jansen,¹ Patricia JTA Groenen,² Astrid Eijkelenboom,² Wendy Stevens,⁴ Corine J Hess,⁴ J Han van Krieken,² Joost SP Vermaat,⁵ Arjen HG Cleven,⁶ Ruben AL de Groen,^{5,6} Viviana Neviani,⁷ Daphne de Jong,³ Sjoerd van Deventer,^{1,+} Blanca Scheijen,^{2,+} and Annemiek B van Spriel ¹

¹Department of Tumor Immunology, Radboud Institute for Molecular Life Sciences, Radboud university medical center, Nijmegen, The Netherlands; ²Department of Pathology, Radboud Institute for Molecular Life Sciences, Radboud university medical center, Nijmegen, The Netherlands; ³Amsterdam UMC-Vrije Universiteit Amsterdam, Department of Pathology and Cancer Center Amsterdam, Amsterdam, The Netherlands; ⁴Department of Hematology, Radboud university medical center, Nijmegen, The Netherlands; ⁵Department of Hematology, Leiden University Medical Center, Leiden, The Netherlands; ⁶Department of Pathology, Leiden University Medical Center, Leiden, The Netherlands; and ⁷Crystal and Structural Chemistry, Department of Chemistry, Bijvoet Center for Biomolecular Research, Utrecht University, Utrecht, The Netherlands.

*S.E, C.M.D.W and M.V.D.B contributed equally to this work.

+ S.V.D. and B.S. contributed equally to this work.

Corresponding author: Annemiek B. van Spriel, Department of Tumor Immunology, Radboud Institute for Molecular Life Sciences, Radboud university medical center, Geert Grooteplein-Zuid 26-28, 6525 GA Nijmegen, The Netherlands. E-mail: Annemiek.vanSpriel@radboudumc.nl; Phone: +31-24-3617600; Fax: +31-24-3540339

Running title: Inactivating *CD37* mutations in IP-DLBCL

Text word count: 1191

Abstract word count: 155

Number of figures: 2

Number of references: 25

Scientific category: Lymphoid Neoplasia

Key points:

- Loss-of-function mutations in *CD37* occur predominantly in diffuse large B-cell lymphoma at immune-privileged sites.
- *CD37*-mutated lymphoma B-cells show impaired CD37 cell surface localization, which may have implications for anti-CD37 therapies.

Abstract

Tetraspanin CD37 is predominantly expressed on the cell surface of mature B-lymphocytes, and is currently being studied as novel therapeutic target for B-cell lymphoma. Recently, we demonstrated that loss of CD37 induces spontaneous B-cell lymphoma in *Cd37*-knockout mice and correlates with inferior survival in patients with diffuse large B-cell lymphoma (DLBCL). Here, *CD37* mutation analysis was performed in a cohort of 137 primary DLBCL, including 44 primary immune-privileged site-associated DLBCL (IP-DLBCL) originating in testis or central nervous system. *CD37* mutations were exclusively identified in IP-DLBCL cases (10/44, 23%), but absent in non-IP-DLBCL cases. The aberrations included ten missense mutations, one deletion, and three splice-site *CD37* mutations. Modeling and functional analysis of *CD37* missense mutations revealed loss-of-function by impaired CD37 protein expression at the plasma membrane of human lymphoma B-cells. This study provides novel insight into the molecular pathogenesis of IP-DLBCL, and indicates that anti-CD37 therapies will be more beneficial for DLBCL patients without *CD37* mutations.

Introduction

Diffuse large B-cell lymphoma (DLBCL) is the most common type of B-cell non-Hodgkin lymphoma (NHL). Several genetic aberrations are known to underlie DLBCL development and progression. Recently, we identified that *Cd37*-knockout mice spontaneously develop B-cell lymphoma.¹ Moreover, CD37 protein expression has been reported to be an independent prognostic factor for patient outcome in R-CHOP (rituximab, cyclophosphamide, doxorubicin, vincristine, prednisone)-treated DLBCL patients.²

CD37 (Tspan-26), a member of the tetraspanin superfamily, is highly expressed on mature B-lymphocytes,³ and is currently studied as novel target for CAR-T cell therapy⁴ and antibody-based therapies for patients with relapsed/refractory NHL.^{5,6} Tetraspanins control the spatial distribution of membrane proteins through specific interactions with (immune-)receptors and signaling molecules, thereby facilitating intracellular signaling pathways.^{7,8} Tetraspanins are associated with different malignancies,⁹ but the role of altered tetraspanin function in DLBCL pathogenesis is unclear.

This study evaluated the mutational status of the human *CD37* gene in DLBCL patients, particularly in DLBCL at immune-privileged sites (IP-DLBCL), including primary testis lymphoma (PTL) and primary central nervous system lymphoma (PCNSL). With functional analysis the effect of identified *CD37* mutations on CD37 protein expression at the cell membrane was studied.

Methods

Cases

The study was conducted with 137 archived primary DLBCL samples, including 44 IP-DLBCL. The discovery cohort included 31 DLBCL samples and 106 DLBCL samples were analyzed in the validation cohort. Samples were collected from multiple Dutch university hospitals (Supplemental Table 1).

Mutation analysis

CD37 mutation analysis of the discovery cohort was performed by amplicon-based sequencing with Ion Torrent and Sanger sequencing. For the validation cohort, single molecule molecular inversion probe (smMIP) mutation analysis and sequencing with Ion Torrent included the *CD37* gene and hotspot loci of *CARD11*, *CD79A*, *CD79B* and *MYD88*.

Functional analysis of mutant *CD37*

The CD37-Gly88Asp-GFP and CD37-Gly65Glu-GFP mutant constructs were generated by introducing point mutations c.263G>A or c.194G>A in hCD37-WT-GFP¹ using site-directed mutagenesis. Human BJAB and OCI-Ly8 lymphoma B-cells were transfected with the AMAXA Nucleofector™ or the Neon™ transfection system, and analyzed for CD37 protein expression and subcellular localization using Western blot and confocal fluorescence microscopy.

Additional experimental details are provided in the supplemental information.

Results and discussion

In a discovery cohort of 31 DLBCL cases, including five PTL, *CD37* mutations were analyzed. *CD37* mutations were identified in two PTL cases, one harboring a missense mutation (c.263G>A (p.Gly88Asp)) and the other a splice-site mutation (c.343-1G>C), but none in the non-IP-DLBCL samples (n=26). To confirm this finding, a validation cohort consisting of 39 IP-DLBCL (18 PTL, 21 PCNSL) and 67 non-IP-DLBCL cases was analyzed for *CD37* mutations along with *CARD11*, *CD79A*, *CD79B* and *MYD88* hotspot mutations (Figure 1; Supplemental Table 2). In this analysis, we also included the five PTL cases from the discovery cohort. Besides confirmation of the two initially identified *CD37* mutations, we uncovered twelve additional mutations (variant allele frequency (VAF) 5.7%-49%; Figure 1B-C). Intriguingly, all *CD37* mutations were exclusively present in IP-DLBCL cases (n=10/44, 23%), and in none of the non-IP-DLBCL cases (n=0/93; Fisher's exact test, $p=0.001$; Figure 1A). Mutation rates of frequently affected genes *CARD11* (5%), *CD79A* (5%), *CD79B* (50%) and *MYD88* (64%) in our cohort (Figure 1B, Supplemental Table 2) were in line with other DLBCL studies.¹⁰⁻¹³ Whole genome and exome sequencing studies of DLBCL report low mutation frequencies of *CD37*, ranging from no mutations to 8%.^{11,14-17}

The *CD37* mutations identified in the validation cohort were detected in eight IP-DLBCL, and included nine missense mutations (c.109C>T (p.Leu37Phe), twice c.194G>A (p.Gly65Glu), c.279G>A (p.Met93Ile), c.279G>T (p.Met93Ile), c.460G>A, (p.Gly154Ser), c.656T>G (p.Val219Gly), c.337G>A (p.Ala113Thr), c.827G>A (p.Arg276Gln)), one in-frame deletion (c.364_399del (p.Val122_Asn133del)), and two splice-site mutations (c.266_267+10del, c.268-2A>C) (Figure 1C; pathogenicity scores in Supplemental Table 2). Within one patient, missense mutation c.194G>A (p.Gly65Glu) was detected in two primary lymphoma specimens as well as healthy control tissue, but not described as a SNP, indicating the presence of a *CD37* germline mutation. To the best of our knowledge, this is the first reported *CD37* germline mutation in humans.

To determine the effect of splice-site mutation c.343-1G>C, cDNA of this DLBCL sample was sequenced, which revealed an 11-base-pair deletion (Supplemental Figure 1). This resulted in a

frame-shift in the *CD37* mRNA sequence leading to a completely altered protein after transmembrane domain 3. Based on previous studies on tetraspanin *CD81* in B cells,¹⁸ this mutation is predicted to result in a non-functional CD37 protein, since the essential extracellular domain 2 (EC2) is truncated.¹⁹ Next, the *CD37* missense mutations and in-frame deletion were mapped onto the reported crystal structure of tetraspanin CD81²⁰ (Supplemental Figure 2). Deletion c.364_399del (p.Val122_Asn133del) disrupts an important structural element of the EC2, namely the A helix, and is therefore also predicted to result in a non-functional CD37 protein.¹⁹

To further assess whether the observed missense mutations resulted in CD37 loss-of-function, we introduced two of the identified *CD37* mutations, c.263G>A (p.Gly88Asp) and c.194G>A (p.Gly65Glu), in human lymphoma B-cells using a green-fluorescent protein (GFP) expression vector. Wild-type CD37 protein appeared as 50-75kD bands on Western blot (Figure 2A-B; Supplemental Figure 3A) due to heavy glycosylation. Protein isoforms with the highest glycosylation state (± 70 kD) were less pronounced in lymphoma B-cells expressing mutant CD37-Gly88Asp-GFP (Figure 2A), and CD37-Gly65Glu-GFP showed a lower molecular weight band on Western blot indicating a glycosylation defect (Figure 2B). Total CD37-GFP protein levels of both mutants were similar to CD37-WT-GFP (Figure 2A-B).

Next, the subcellular localization of the CD37 mutants was determined using confocal microscopy. Lymphoma B-cells expressing the CD37-GFP mutants had significantly lower cell membrane expression and more retention of intracellular CD37 protein compared to cells expressing CD37-WT-GFP (Figure 2C; Supplemental Figure 3B). Moreover, CD37-Gly88Asp had a dominant-negative effect on the membrane expression of CD37-WT protein (Supplemental Figure 4). These data indicate that these missense mutations result in defective glycosylation and trafficking of CD37 in human lymphoma B-cells, which corresponds with the reported role of glycosylation as sorting signal for protein transport to the plasma membrane.²¹ Moreover, modification of cell surface proteins by defective glycosylation frequently contributes to cancer development by enhancing invasive growth and tumor cell migration.²²

We previously showed that loss of CD37 results in increased interleukin-6 (IL-6) signaling and STAT3 activation,¹ which are both known to be involved in the pathogenesis of hematological malignancies.²³ *MYD88* mutations also stimulate cell survival by promoting JAK/STAT3 signaling and IL-6 secretion, suggesting a similar phenotype.²⁴ As proposed for *MYD88* and *CD79B* mutations in IP-DLBCL,¹² mutations in *CD37* could therefore provide a survival advantage in the otherwise stimulus-poor environment of immune-privileged sites.

Seven-out-of-nine evaluable cases with a *CD37* mutation did not express CD37 protein (Supplemental Figure 5, Supplemental Table 1). Since immunohistochemistry does not distinguish between cell surface and cytosolic expression, the importance of CD37 in DLBCL biology^{1,2} is likely underestimated. Moreover, the recent identification of loss of CD19 expression as mechanism underlying disease relapse upon CD19 CAR-T cell therapy,²⁵ emphasizes the need for investigating CD37 surface expression in hematologic malignancies prior to the use of novel CD37 CAR-T cell therapies.

In conclusion, inactivating *CD37* mutations occur predominantly in IP-DLBCL and lead to aberrant CD37 cell surface expression. This study provides novel molecular insight into DLBCL at immune-privileged sites, and indicates that CD37-based therapies are more likely to be beneficial for DLBCL patients that harbor no *CD37* mutations.

Acknowledgements

We thank Piet Gros (Department of Chemistry, Utrecht University) for his valuable help with the modeling studies, and Shannon van Lent-van Vliet and Sanne Sweegers (Department of Pathology, Radboudumc) for their valuable help with the smMIP analysis. S.E. is supported by a Radboudumc PhD grant. C.M.D.W. is supported by a Rubicon Fellowship from the Netherlands Organization for Scientific Research (019.162LW.004). J.V., A.C. and R.G. are supported by research funding from 'Stichting Fonds Oncologie Holland'. A.B. van Spriel is recipient of a Netherlands Organization for Scientific Research Grant (NWO-ALW VIDI grant 864.11.006), a NWO Gravitation Programme 2013 grant (ICI-024.002.009), a Dutch Cancer Society grant (KUN2014-6845), and was awarded an European Research Council Consolidator Grant (Secret Surface, 724281). We apologize to all authors whose work could not be cited due to space limitations.

Authorship contributions

SE, CMDW, MVDB, SVD, BS and ABVS designed the study. SE, CMDW, MVDB, SVD and ABVS wrote the manuscript. MVDB, CH, WS, MGR, DDJ, JV, AC and BS collected DLBCL tissues and corresponding pathological information. SE, CMDW, MVDB, EJ, AVDS, SVD, PJTAG, AE, RG and MB performed mutation analysis. SE, FA, LJ and SVD performed functional *in vitro* experiments. VN performed CD37 modeling studies. JHVK, SVD, BS and ABVS supervised the work.

Conflict of interest

All authors declare no conflict of interest.

References

1. Winde CM de, Veenbergen S, Young KH, et al. Tetraspanin CD37 protects against the development of B cell lymphoma. *J. Clin. Invest.* 2016;126(2):653–666.
2. Xu-Monette ZY, Li L, Byrd JC, et al. Assessment of CD37 B-cell antigen and cell-of-origin significantly improves risk prediction in diffuse large B-cell lymphoma. *Blood.* 2016;128(26):3083–3101.
3. Barrena S, Almeida J, Yunta M, et al. Aberrant expression of tetraspanin molecules in B-cell chronic lymphoproliferative disorders and its correlation with normal B-cell maturation. *Leukemia.* 2005;19(8):1376–83.
4. Scarfò I, Ormhøj M, Frigault MJ, et al. Anti-CD37 chimeric antigen receptor T cells are active against B- and T-cell lymphomas. *Blood.* 2018;132(14):1495–1506.
5. Robak T, Hellmann A, Kloczko J, et al. Randomized phase 2 study of otlertuzumab and bendamustine versus bendamustine in patients with relapsed chronic lymphocytic leukaemia. *Br. J. Haematol.* 2017;176(4):618–628.
6. Stathis A, Flinn IW, Madan S, et al. Safety, tolerability, and preliminary activity of IMG529, a CD37-targeted antibody-drug conjugate, in patients with relapsed or refractory B-cell non-Hodgkin lymphoma: a dose-escalation, phase I study. *Invest. New Drugs.* 2018;36(5):869–876.
7. Rubinstein E, Le Naour F, Lagaudriere-Gesbert C, et al. CD9, CD63, CD81, and CD82 are components of a surface tetraspan network connected to HLA-DR and VLA integrins. *Eur J Immunol.* 1996;26(11):2657–2665.
8. Zuidsherwoude M, Göttfert F, Dunlock VME, et al. The tetraspanin web revisited by super-resolution microscopy. *Sci. Rep.* 2015;5(1):12201.
9. Hemler ME. Tetraspanin proteins promote multiple cancer stages. *Nat. Rev. Cancer.* 2014;14(1):49–60.
10. Reddy A, Zhang J, Davis NS, et al. Genetic and Functional Drivers of Diffuse Large B Cell Lymphoma. *Cell.* 2017;171(2):481-494.e15.

11. Chapuy B, Stewart C, Dunford AJ, et al. Molecular subtypes of diffuse large B cell lymphoma are associated with distinct pathogenic mechanisms and outcomes. *Nat. Med.* 2018;24(5):679–690.
12. Kraan W, Horlings HM, van Keimpema M, et al. High prevalence of oncogenic MYD88 and CD79B mutations in diffuse large B-cell lymphomas presenting at immune-privileged sites. *Blood Cancer J.* 2013;3(9):e139.
13. Bruno A, Boisselier B, Labreche K, et al. Mutational analysis of primary central nervous system lymphoma. *Oncotarget.* 2014;5(13):5065–5075.
14. Zhang J, Grubor V, Love CL, et al. Genetic heterogeneity of diffuse large B-cell lymphoma. *Proc. Natl. Acad. Sci. U. S. A.* 2013;110(4):1398–403.
15. Morin RD, Mungall K, Pleasance E, et al. Mutational and structural analysis of diffuse large B-cell lymphoma using whole-genome sequencing. *Blood.* 2013;122(7):1256–65.
16. Park HY, Lee S-B, Yoo H-Y, et al. Whole-exome and transcriptome sequencing of refractory diffuse large B-cell lymphoma. *Oncotarget.* 2016;7(52):86433–86445.
17. Schmitz R, Wright GW, Huang DW, et al. Genetics and Pathogenesis of Diffuse Large B-Cell Lymphoma. *N. Engl. J. Med.* 2018;378(15):1396–1407.
18. Vences-Catalán F, Kuo C-C, Sagi Y, et al. A mutation in the human tetraspanin CD81 gene is expressed as a truncated protein but does not enable CD19 maturation and cell surface expression. *J. Clin. Immunol.* 2015;35(3):254–263.
19. Stipp CS, Kolesnikova T V, Hemler ME. Functional domains in tetraspanin proteins. *Trends Biochem. Sci.* 2003;28(2):106–12.
20. Zimmerman B, Kelly B, McMillan BJ, et al. Crystal Structure of a Full-Length Human Tetraspanin Reveals a Cholesterol-Binding Pocket. *Cell.* 2016;167(4):1041-1051.e11.
21. Lodish H, Berk A, Kaiser CA, et al. Moving proteins into membranes and organelles. *Mol. Cell Biol. 8th edn.* 2016;583–630.
22. Gill DJ, Tham KM, Chia J, et al. Initiation of GalNAc-type O-glycosylation in the endoplasmic

- reticulum promotes cancer cell invasiveness. *Proc. Natl. Acad. Sci. U. S. A.* 2013;110(34):E3152-61.
23. Burger R. Impact of Interleukin-6 in Hematological Malignancies. *Transfus. Med. Hemotherapy.* 2013;40(5):336–343.
24. Ngo VN, Young RM, Schmitz R, et al. Oncogenically active MYD88 mutations in human lymphoma. *Nature.* 2011;470(7332):115–119.
25. Orlando EJ, Han X, Tribouley C, et al. Genetic mechanisms of target antigen loss in CAR19 therapy of acute lymphoblastic leukemia. *Nat. Med.* 2018;24(10):1504–1506.

Figure legends

Figure 1. High frequency of mutated *CD37* in IP-DLBCL. (A) Frequency of *CD37* mutations in non-IP-DLBCL versus IP-DLBCL. The total number of lymphoma cases for each group is indicated. Numbers in the *CD37* mutation row indicate the number of lymphoma cases carrying one or more *CD37* mutations. IP-DLBCL = immune-privileged site-associated diffuse large B-cell lymphoma. *P* = statistical significance obtained using Fisher's exact test. (B) OncoPrint (left) and Venn diagram (right) show the frequencies of *CD37*, *CARD11*, *CD79A*, *CD79B* and *MYD88* mutations in all IP-DLBCL studied (23 PTL and 21 PCNSL cases). Columns show individual tumors. Asterisk indicates samples from the same patient containing the *CD37* germline mutation. Genetic details per mutation can be found in Supplementary Table 2. PTL = primary testis lymphoma, PCNSL = primary central nervous system lymphoma, green = missense mutation, black = splice-site mutation, magenta = deletion, grey = no mutation. (C) Schematic representation of mutations detected in the *CD37* gene. Dark grey boxes represent the coding sequence of *CD37*, light grey boxes are the non-coding sequence before exon 1 (begin) and after exon 8 (end), and black lines represent introns. Asterisk indicates the *CD37* germline mutation.

Figure 2. Mutations in *CD37* cause aberrant *CD37* glycosylation and localization. Western blot analysis of *CD37* protein expression in BJAB lymphoma B-cells transfected with *CD37*-WT-GFP, *CD37*-Gly88Asp-GFP (A) or *CD37*-Gly65Glu-GFP (B). Blots were probed with α -GFP to detect *CD37*-GFP expression (50-75kD; upper blot). α -Tubulin was used as a loading control (lower blot). Protein expression level of *CD37*-mutant-GFP was normalized to *CD37*-WT-GFP for each experiment (n=3). ns: $p=0.73$ (left), $p=0.96$ (right), paired t-test. (C) Confocal microscopy images of BJAB cells expressing *CD37*-WT-GFP and *CD37*-Gly88Asp-GFP or *CD37*-Gly65Glu-GFP (green) co-stained for MHC-I (red) to identify the plasma membrane. Overview images (top) and single cell images (bottom left) show representative cells of three independent experiments for both *CD37*-WT-GFP and *CD37*-mutant-GFP. Scale bar = 10 μ m. Ratio between membrane and cytoplasmic GFP expression was quantified from 10

representative cells of three independent experiments. * $p=0.023$ (left), $p=0.011$ (right), paired t-test.

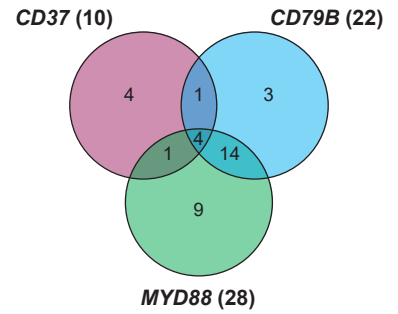
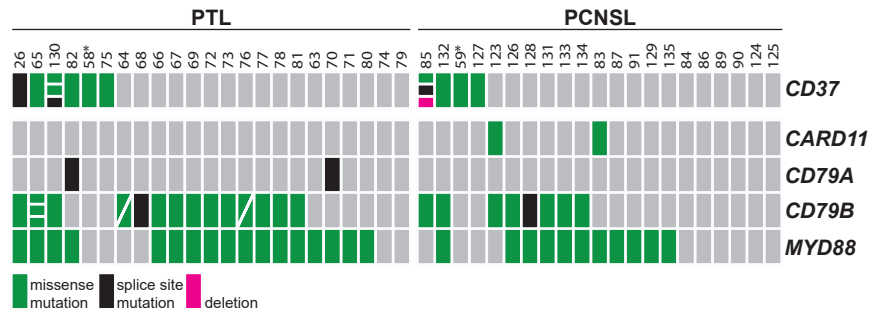
All data represent mean \pm SEM.

Figure 1

A

	Non-IP-DLBCL n=93	IP-DLBCL n=44	<i>P</i>
CD37 mutation	0	10	0.0001

B



C

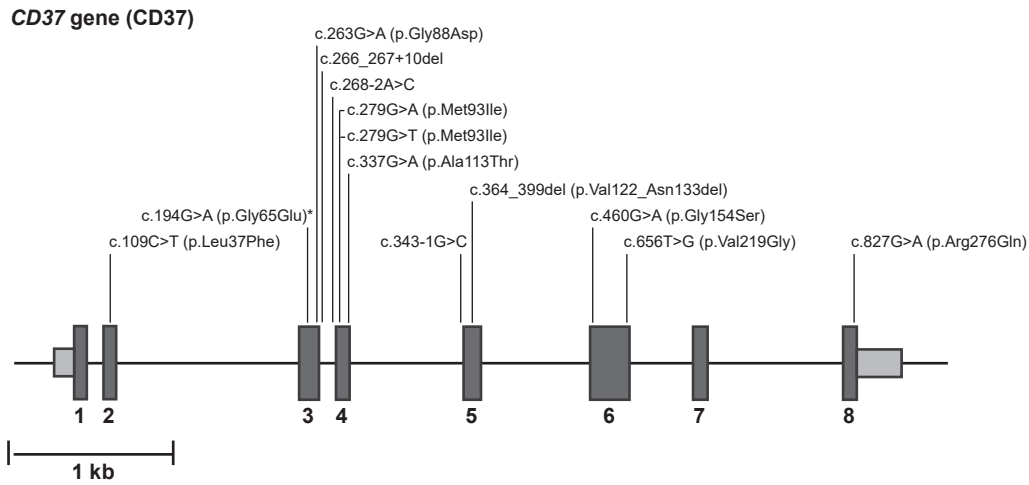


Figure 2

